



# Climatic Impacts of Wind Power

## Citation

Miller, Lee M. and David W. Keith. "Climatic impacts of wind power." *Joule* 2, no. 12 (2018): 2618-2632. doi: 10.1016/j.joule.2018.09.009

## Permanent link

<http://nrs.harvard.edu/urn-3:HUL.InstRepos:42662010>

## Terms of Use

This article was downloaded from Harvard University's DASH repository, and is made available under the terms and conditions applicable to Other Posted Material, as set forth at <http://nrs.harvard.edu/urn-3:HUL.InstRepos:dash.current.terms-of-use#LAA>

## Share Your Story

The Harvard community has made this article openly available.  
Please share how this access benefits you. [Submit a story](#).

[Accessibility](#)

**Title: Climatic impacts of wind power**

**Authors:** Lee M. Miller<sup>1,\*</sup>, David.W. Keith<sup>1,2</sup>

**Affiliations:**

<sup>1</sup>School of Engineering and Applied Sciences, Harvard University, Cambridge, MA 02139, USA

<sup>2</sup> Harvard Kennedy School, Cambridge, MA 02138, USA

\*Correspondence to: lmiller@seas.harvard.edu

**Abstract:** We simulate the climatic impacts of large-scale wind power over the US using a high-resolution mesoscale model. The diurnal and seasonal cycle of the climate response to wind power is roughly consistent with recent observations of the climate impacts of wind farms. A scenario that generates 0.46 TW<sub>e</sub> of wind energy over the windiest 1/3 of the US warms the Continental US by an average 0.24°C. This impact is negligible compared to estimated 21<sup>st</sup> century warming, yet it would take more than a century before wind's warming impacts are offset by the climate benefits of reduced emissions. The ratio of climate-impact to climate-benefit is much smaller for solar PV. Wind's overall environmental impacts are surely less than fossil energy, yet quantifying wind's climate impacts are relevant to informing choices between low carbon energy sources during the transition to a decarbonized energy system.

**One Sentence Summary:** Observations and models suggest that wind power causes climate changes that are large compared to some other low-carbon renewables such as solar.

**Main Text:**

Wind turbines generate electricity by extracting kinetic energy, which slows winds and modifies the exchange of heat, moisture, and momentum between the surface and the atmosphere. Observations show that wind turbines alter local climate (*I–10*), and models show local- to global-scale climate changes from the large-scale extraction of wind power (*11–15*). Yet the extent to which future wind power deployment will alter climate is uncertain. How does wind's climate impact per unit energy production compare to the climate impacts of other low-carbon technologies? Does wind power's climatic impact matter? Current analysis does not provide policy-relevant answers to such questions.

Wind turbines increase vertical transport by adding turbulence to the atmospheric boundary layer (ABL). The impact of added turbulence on climate may be strongest at night when the ABL is thin (<100m) and the vertical temperature profile is steep, causing turbine-induced mixing to

transport warmer air downward. This mechanism may explain recent observations of warmer nighttime surface temperatures near operating wind farms (Table 1).

Climatic impacts due to wind power extraction were first studied using general circulation models (GCMs). These studies found statistically significant climatic impacts within the wind farm, as well as long-distance teleconnections, with impacts outside the wind farm sometimes as large in magnitude as impacts inside the wind farm (11–13, 16). Note that such impacts are unlike greenhouse gas (GHG) driven warming, as in some cases wind power's climatic impacts might counteract such GHG warming—at least four studies have found that mid-latitude wind power extraction can cool the Arctic (11, 12, 17, 18). However, these studies often used idealized or unrealistic distributions of turbines installed at unrealistic scales. Model simulations of geometrically simple, isolated wind farms at smaller scales of 3,000–300,000 km<sup>2</sup> (10- to 1000-times larger than today's wind farms) in windy locations found substantial reductions in wind speed and changes in atmospheric boundary layer (ABL) thickness, as well as differences in temperature (11, 13, 14, 19), precipitation (14, 20), and vertical atmospheric exchange (15, 21).

We want to assess wind power's climate impacts per unit of energy generation, yet wind's climatic impacts depend on local meteorology and on non-local climate teleconnections. These twin dependencies mean that wind power's impacts are strongly dependent on the amount and location of wind power extraction, frustrating the development of a simple impact metric.

As a step towards an improved policy-relevant understanding, we explore the climatic impacts of generating 0.46 TW<sub>e</sub> of wind-derived electricity over the Continental US. This scale fills a gap between the smaller isolated wind farms and global-scale GCM. We model a uniform turbine density within the windiest 1/3 of the Continental US, and vary the density parametrically.

Our 0.46 TW<sub>e</sub> *benchmark scenario* is ~18 times the 2016 US wind power generation rate (22). We intend it as a plausible scale of wind power generation if wind power plays a major role in decarbonizing the energy system in the latter half of this century. For perspective, the benchmark's generation rate is only 14% of US current primary energy consumption (23), about the same as US electricity consumption (22), and about 2.4 times larger than the projected 2050 US wind power generation rate of the *Central Study* in NREL's recent *Wind Vision* (24). Finally, it is less than 1/6<sup>th</sup> the technical wind power potential over the same windy areas of the US as estimated by (24, 25).

## Modeling framework

We use the WRF v3.3.1 high-resolution regional model (26) with a domain that encompasses the Continental US, forced by boundary conditions from the North American Regional Reanalysis (27). The *wind farm region* is more than 500 km from the model boundaries, and encompasses only 13% of the domain (shown in Fig. 1A). The model configuration used dynamic soil moisture and 31 vertical levels with 3 levels intersecting the turbine's rotor and 8 levels representing the lowermost kilometer. The model is run for a full year after a one-month spin-up using horizontal resolutions of 10 and 30 km. The wind turbine parametrization is based on the thrust and power coefficients of a Vestas 3 MW turbine, and is very similar to previous modeling studies (14, 15, 19).

The advantage of the regional model is that we can use a horizontal and vertical resolution substantially higher than previous global modeling studies (11–13, 16–18, 21, 28), allowing better representation of the interactions of the wind turbines with the ABL. The disadvantage of using prescribed boundary conditions is that our simulations will underestimate the climatic response to wind power extraction compared to a global model with equivalent resolution, which would allow the global atmosphere to react to the increased drag over the U.S. and would reveal climate teleconnections.

We tested horizontal resolution dependence by comparing the 10 and 30 km simulations with a turbine density of  $3.0 \text{ MW km}^{-2}$  to the respective 2012 controls. Differences in the annual average 2-meter air temperature were small, as shown in Fig. S1. The following results use a 30 km resolution (about 1/9 the computational expense) and 2012, 2013, and 2014 simulation periods to reduce the influence of interannual variability. We use four turbine densities (0.5, 1.0, 1.5,  $3.0 \text{ MW km}^{-2}$ ) within the wind farm region to explore how increased wind power extraction rates alter the climatic impacts.

## Results

Figure 1 shows the climate impacts of the benchmark scenario. The wind farm region experiences warmer average temperatures (Fig. 1A), with about twice the warming effect at night compared to during the day (Fig. 1B and C). The climate response is concentrated in the wind farm region, perhaps because teleconnections are suppressed by the boundary conditions. Changes in precipitation are small and show no clear spatial correlation (Fig. S2). The warming is greatest in a N-S corridor near the center of the wind turbine array, perhaps because of an interaction between wind turbines and the nocturnal low-level jet (LLJ). The LLJ is a fast nocturnal low-altitude wind ( $>12 \text{ ms}^{-1}$  at 0.5 km) common in the US Midwest which occurs when the atmosphere decouples from surface friction, resulting in a steep vertical temperature gradient (29)—meteorological conditions that might be sensitive to perturbations by wind turbines. We quantified the presence of the LLJ in our control simulation but do not find strong spatial agreement between the probability of LLJ occurrence and the nighttime warming (Fig. S4).

Warming and power generation saturate with increasing turbine density (Fig. 2). The temperature saturation is sharper, so the ratio of temperature change per unit energy generation decreases with increasing turbine density. This suggests that wind's climate impacts per unit energy generation may be somewhat larger for lower values of total wind power production.

Power generation appears to approach the wind power generation limit at turbine densities somewhat above the maximum we explored. The highest ( $3.0 \text{ MW km}^{-2}$ ) turbine density yields an areal (surface) power generation of  $0.70 \text{ W}_e \text{ m}^{-2}$ , consistent with some previous studies (15–17, 19, 21), but half the  $1.4 \text{ W}_e \text{ m}^{-2}$  assumed possible by 2050 from the same  $3.0 \text{ MW km}^{-2}$  turbine density into windy regions by (24). While we did not compute a maximum wind power generation rate here, extrapolation of Fig. 2 suggests that it is about  $2 \text{ TW}_e$ , significantly less than the  $3.7 \text{ TW}_e$  of technical potential estimated by (24, 25) over less land area. Clearly,

interactions of wind turbines with climate must be considered in estimates of technical wind power potential.

### **Interpretation**

The climatic impacts of wind power may be unexpected, as wind turbines only redistribute heat within the atmosphere, and the  $1.0 \text{ W m}^{-2}$  of heating resulting from kinetic energy dissipation in the lower atmosphere is only about 0.6% of the diurnally-averaged radiative flux. But wind's climatic impacts are not caused by additional heating from the increased dissipation of kinetic energy. Impacts arise because turbine-atmosphere interactions alter surface-atmosphere fluxes, inducing climatic impacts that may be much larger than arise from the direct impact of the dissipation energy flux alone.

As wind turbines extract kinetic energy from the atmospheric flow and slow wind speeds, the vertical gradient in wind speed steepens, and downward entrainment increases (15). These interactions increase the mixing between air from above and air near the surface. The strength of these interactions depends on the meteorology, and in particular the diurnal cycle of the ABL.

During the daytime, solar-driven convection mixes the atmosphere to heights of 1-3 km (29). Wind turbines operating during the daytime are enveloped within this already well-mixed air, so climatic impacts such as daytime temperature differences are therefore generally quite small. At night, radiative cooling results in stable surface conditions, with about 100-300 m of stable air separating the influence of surface friction from the winds aloft (29). Wind turbines operating at night, with physical extents of 100-150 m and an influence height at night reaching 500 m or more (15), can entrain warmer (potential temperature) air from above down into the previously stable and cooler (potential temperature) air near the surface, warming surface temperatures. In addition to the direct mixing by the turbine wakes, turbines reduce the wind speed gradient below their rotors and thus sharpen the gradient aloft. This sharp gradient may then generate additional turbulence and vertical mixing.

This explanation is broadly consistent with the strong day-night contrast of our benchmark scenario (Fig. 1B and 1C). Within the wind farm region during the day, most locations experience warmer air temperatures, although ~15% of locations show a daytime cooling effect in July-September. At night during July-September, less than 5% of locations show a cooling effect, and the warming effect at night over all months is much larger than during the daytime. This daytime and nighttime warming effect is also larger with higher turbine densities (Fig. S3). Finally, the temperature perturbation in the benchmark scenario shows a strong correlation to differences in turbulent kinetic energy (TKE) within 56 m of the ground (Fig. 1D), supporting the explanation that the temperature response is driven by increased vertical mixing.

### **Observational evidence of climatic impacts**

While numerous observational studies have linked wind power to reduced wind speeds and increased turbulence in the turbine wakes (1, 4, 7, 30, 31), ten studies have quantified the climatic impacts resulting from these changes (Table 1).

Three ground-based studies have measured differences in surface temperature (1, 5, 7) and evaporation (5). Generally, these ground-based observations show minimal climatic impacts during the day, but increased temperatures and evaporation rates at night.

Seven satellite-based studies have quantified surface (skin) temperature differences. By either comparing time periods before and after turbine deployment, or by comparing areas upwind, inside, and downwind of turbines, the spatial extent and intensity of warming for 28 operational wind farms in California (32), Illinois (6), Iowa (2), and Texas (8–10) has been observed. There is substantial consistency between these satellite observations despite the diversity of local meteorology and wind farm deployment scales. Daytime temperature differences were small and slightly warmer and cooler, while nighttime temperature differences were larger and almost always warmer (Table 1). Interpretation of the satellite data is frustrated by its generally fixed overpass times and clouds obscuring the surface.

Although our benchmark scenario is very different in scale and turbine placement compared to operational wind power, it is nevertheless instructive to compare our simulation with observations. We compare results at a single Texas location (100.2°W, 32.3°N) where one of the world's largest clusters of operational wind turbines (~200 km<sup>2</sup>, consisting of open space and patchy turbine densities of 3.8–4.7 MW km<sup>-2</sup> (33)) has been linked to differences in surface temperature in 3 of the observational studies in Table 1. Weighting the observations by the number of observed-years, the Texas location is 0.01°C warmer during the day and 0.29°C warmer at night. Our benchmark scenario with a uniform turbine density of 0.5 MW km<sup>-2</sup> at this location is 0.33°C warmer during the day and 0.66°C warmer at night. To explore the quantitative correlation between the seasonal and diurnal response, we take the 8 seasonal day and night values as independent pairs (Supp. Table S1), and find that the observations and the simulations are strongly correlated (Figure 3). This agreement provides strong evidence that the physical mechanisms being modified by the deployment of wind turbines are being captured by our model.

## Limitations

We assumed that turbines were evenly spaced over the whole wind farm region. Real turbine deployment is patchier—wind farms with turbine densities of several MW km<sup>-2</sup> are interspersed among areas with no turbines. Would a patchy arrangement of individual wind farms cause similar climatic impacts if it operated within the same wind farm region with the same average turbine density?

Climate response is partly related to the specific choice of wind turbine. We modeled a specific 3.0 MW turbine, but future deployment may shift to wind turbines with taller hub-heights and larger rotor-diameters, changing the turbine-atmosphere-surface interactions.

The model's boundary conditions are prescribed and do not respond to changes caused by wind turbines. Yet prior work has established that non-local climate responses to wind power may be significant (12), suggesting that the impacts of our benchmark would be larger if simulated using a global setup. The 3-year simulation period was also completed in 1-year blocks, so we do not simulate the response of longer-term climate dynamics determined by variables such as soil moisture. Finally, model resolution influenced the estimated climatic impacts. Simulations with a

10 km horizontal resolution and the highest turbine density of  $3.0 \text{ MW km}^{-2}$  caused 18% less warming than the 30 km simulation ( $+0.80$  and  $+0.98^\circ\text{C}$ ). Simulations using a global model with an unequally spaced grid with high-resolution over the US could resolve some of these uncertainties.

### Comparing climatic impacts to climatic benefits

Environmental impacts of energy technologies are often compared by estimating impacts per unit energy production, such as the air pollution mortality per unit power generation (34). One could compute similar metrics when considering the climate impact of low-carbon energy technologies like wind power. Alternatively, since the central benefit of low-carbon energy is reduced climate change, it is possible to make dimensionless climate-to-climatic comparisons between the climate impacts and climate benefits of reduced emissions.

When wind power replaces fossil energy, it cuts  $\text{CO}_2$  emissions, reducing greenhouse gas driven global climate change, while at the same time causing climatic impacts as described above and elsewhere (1–16, 18–21, 28, 32, 35–37). These climatic impacts differ in (at least) three important dimensions. First, the direct climatic impact of wind power is immediate but would disappear if the turbines were removed, while the climatic benefits of reducing emissions grows with the cumulative reduction in emissions and persists for millennia. Second, the direct climatic impacts of wind power are predominantly local to the wind farm region, while the benefits of reduced emissions are global. Third, the direct impacts of wind power are spatially and temporally variable, whereas the climatic benefits of reducing emissions are global and far more uniform.

As a step towards a climate-impact to climate-benefit comparison for wind, we compare warming over the US. We begin by assuming that US wind power generation increases linearly from the current level to  $0.46 \text{ TW}_e$  in 2080 and is constant thereafter. We estimate the associated warming by scaling our benchmark scenario's temperature differences linearly with wind power generation. The amount of avoided emissions—and thus the climate benefit—depends on the emissions intensity of the electricity that wind displaces. We bracket uncertainties in the time evolution of the carbon-intensity of US electric power generation in the absence of wind-power by using two pathways. One pathway assumes a static emissions intensity at the 2016 value ( $0.44 \text{ kgCO}_2 \text{ kWh}^{-1}$ ), while the second pathway's emissions intensity decreases linearly to zero at 2100, which is roughly consistent with the GCAM model (38) that meets the IPCC RCP4.5 scenario. The two emissions pathways are then reduced by the (zero emission) wind power generation rate at that time (Fig. 4C). The first pathway likely exaggerates wind power's emission reductions, while the second reflects reduced benefit for wind in a transition to a zero-carbon grid that might be powered by solar or nuclear.

We estimate wind's reduction in global warming by applying these two emission pathways to an emissions-to-climate impulse response function (39). We convert these global results to a US warming estimate using a ratio of US-to-global warming from IPCC RCP4.5 and RCP8.5 ensemble means (Fig. S5, (40)).

The benchmark scenario's warming of  $0.24^\circ\text{C}$  over the Continental US and  $0.54^\circ\text{C}$  over the wind farm region are both small and large depending on the baseline. Climatic impacts are small in

comparison to US temperature projections— historical and ongoing global emissions are projected to cause about 0.24°C of US warming by the year 2030 (Fig. S5). Climatic impacts are large in comparison to the short- to medium-term benefit of reduced US electricity emissions, particularly within the wind farm region where the climate impacts of wind power are both immediate and substantially larger than the climate benefits due to emissions reductions (Fig. 4). Yet the climate benefits are global so—as with many energy decisions—local impacts must be set against global benefits.

### Implications for energy system decarbonization

Wind beats fossil fuels under any reasonable measure of long-term environmental impacts per unit of energy. Assessing the environmental impacts of wind power is relevant because, like all energy sources, wind power causes environmental impacts. As society decarbonizes energy systems to limit climate change, policy makers will confront trade-offs between various low-carbon energy technologies such as wind, solar, biofuels, nuclear, and fossil fuel with carbon capture. Each technology benefits the global climate by reducing carbon emissions, but each technology also causes local environmental impacts.

A study of solar power also found climate impacts (41). We compare wind and solar by estimating warming from solar PV using values from (41) and the method described above. Solar PV causes a warming effect that is 7 to 10 times smaller than wind's (Fig 4D). This contrast may arise, in part, from the difference in spatial area required to generate power—today's solar farms can generate 10 to 20 Wm<sup>-2</sup>, while wind power is limited to about 1 Wm<sup>-2</sup>. We also speculate that solar PV's climatic impacts might be reduced by modifying the siting or technology, but these aspects causing wind's climatic impacts are more difficult to modify.

This study, along with observations and prior model-based analysis, suggests that wind power may cause non-negligible climate impacts. There is no simple answer regarding the *best* renewable technology, but choices between renewable energy sources should be informed by systematic analysis of their environmental impacts.

### References:

1. S. Baidya Roy, J. J. Traiteur, Impacts of wind farms on surface air temperatures. *Proc. Natl. Acad. Sci. U.S.A.* **107**, 17899–17904 (2010).
2. R. A. Harris, L. Zhou, G. Xia, Satellite observations of wind farm impacts on nocturnal land surface temperature in Iowa. *Remote Sens.* **6**, 12234–12246 (2014).
3. C. B. Hasager *et al.*, Using satellite SAR to characterize the wind flow around offshore wind farms. *Energies*. **8**, 5413–5439 (2015).
4. D. A. Rajewski *et al.*, Crop Wind Energy Experiment (CWEX): Observations of Surface-Layer, Boundary Layer, and Mesoscale Interactions with a Wind Farm. *Bull. Am. Meteorol. Soc.* **94**, 655–672 (2013).
5. D. A. Rajewski *et al.*, Changes in fluxes of heat, H<sub>2</sub>O, and CO<sub>2</sub> caused by a large wind farm. *Agric. For. Meteorol.* **194**, 175–187 (2014).

- 313 6. L. M. Slawsky *et al.*, Observed Thermal Impacts of Wind Farms Over Northern Illinois. *Sensors*. **15**, 14981–  
314 15005 (2015).
- 315 7. C. Smith, R. J. Barthelmie, S. C. Pryor, In situ observations of the influence of a large onshore wind farm on  
316 near-surface temperature, turbulence intensity and wind speed. *Environ. Res. Lett.* **8**, 034006 (2013).
- 317 8. G. Xia, L. Zhou, J. Freedman, S. Roy, A case study of effects of atmospheric boundary layer turbulence, wind  
318 speed, and stability on wind farm induced temperature changes using observations from a field. *Clim. Dyn.*  
319 **46**, 2179–2196 (2016).
- 320 9. L. Zhou, Y. Tian, S. Baidya Roy, Y. Dai, H. Chen, Diurnal and seasonal variations of wind farm impacts on  
321 land surface temperature over western Texas. *Clim. Dyn.* **41**, 307–326 (2013).
- 322 10. L. Zhou *et al.*, Impacts of wind farms on land surface temperature. *Nat. Clim. Change*. **2**, 539–543 (2012).
- 323 11. D. W. Keith *et al.*, The influence of large-scale wind power on global climate. *Proc. Natl. Acad. Sci. U.S.A.*  
324 **101**, 16115–16120 (2004).
- 325 12. D. Kirk-Davidoff, D. W. Keith, On the Climate Impact of Surface Roughness Anomalies. *J. Atmos. Sci.* **65**,  
326 2215–2234 (2008).
- 327 13. C. Wang, R. G. Prinn, Potential climatic impacts and reliability of very large-scale wind farms. *Atmos. Chem.*  
328 *Phys.* **10**, 2053–2061 (2010).
- 329 14. R. Vautard *et al.*, Regional climate model simulations indicate limited climatic impacts by operational and  
330 planned European wind farms. *Nat. Commun.* **5**, 1–9 (2014).
- 331 15. L. M. Miller *et al.*, Two methods for estimating limits to large-scale wind power generation. *Proc. Natl. Acad.*  
332 *Sci. U.S.A.* **112**, 11169–74 (2015).
- 333 16. L. M. Miller, F. Gans, A. Kleidon, Estimating maximum global land surface wind power extractability and  
334 associated climatic consequences. *Earth Syst. Dyn.* **2**, 1–12 (2011).
- 335 17. M. Z. Jacobson, C. L. Archer, Saturation wind power potential and its implications for wind energy. *Proc.*  
336 *Natl. Acad. Sci. U.S.A.* **109**, 15679–84 (2012).
- 337 18. K. Marvel, B. Kravitz, K. Caldeira, Geophysical limits to global wind power. *Nat. Clim. Change*. **2**, 1–4  
338 (2012).
- 339 19. A. S. Adams, D. W. Keith, Are global wind power resource estimates overstated? *Environ. Res. Lett.* **8**,  
340 015021 (2013).
- 341 20. B. H. Fiedler, M. S. Bukovsky, The effect of a giant wind farm on precipitation in a regional climate model.  
342 *Environ. Res. Lett.* **6**, 045101 (2011).
- 343 21. L. M. Miller, A. Kleidon, Wind speed reductions by large-scale wind turbine deployments lower turbine  
344 efficiencies and set low generation limits. *Proc. Natl. Acad. Sci. U.S.A.*, 13570–75 (2016).
- 345 22. US Energy Information Administration, Electric power monthly. EIA Publication, 2017;  
346 [www.eia.gov/electricity/monthly/pdf/epm.pdf](http://www.eia.gov/electricity/monthly/pdf/epm.pdf)
- 347 23. US Energy Information Administration, U.S. primary energy consumption by source and sector, 2016. EIA  
348 Publication, 2017; [www.eia.gov/totalenergy/data/monthly/pdf/flow/css\\_2016\\_energy.pdf](http://www.eia.gov/totalenergy/data/monthly/pdf/flow/css_2016_energy.pdf)

24. US Dept. of Energy, Wind Vision: a new era for wind power in the United States. DOE Publication, 2015; [www.energy.gov/sites/prod/files/WindVision\\_Report\\_final.pdf](http://www.energy.gov/sites/prod/files/WindVision_Report_final.pdf)
25. A. Lopez *et al.*, U.S. renewable energy technical potentials: a GIS-based analysis. DOE Tech. Rep. TP-6A20-51946, 2012; [www.nrel.gov/docs/fy12osti/51946.pdf](http://www.nrel.gov/docs/fy12osti/51946.pdf)
26. W. C. Skamarock *et al.*, A description of the advanced research WRF version 3. NCAR technical note NCAR/TN-475+STR (National Center for Atmospheric Research, Boulder, CO)
27. F. Mesinger *et al.*, North American Regional Reanalysis. *Bull. Am. Meteorol. Soc.* **87**, 343–360 (2006).
28. D. B. Barrie, D. B. Kirk-Davidoff, Weather response to management of a large wind turbine array. *Atmos. Chem. Phys.*, **10**, 769–775 (2010).
29. J. R. Garratt, *The Atmospheric Boundary Layer*, Cambridge University Press (1994).
30. B. D. Hirth *et al.*, Measuring a utility-scale turbine wake using the ttuka mobile research radars. *J. Atmospheric Ocean. Technol.* **29**, 765–771 (2012).
31. G. V. Iungo, Y. Wu, F. Porté-Agel, Field Measurements of Wind Turbine Wakes with Lidars. *J. Atmospheric Ocean. Technol.*, 274–287 (2013).
32. J. M. Walsh-Thomas *et al.*, Further evidence of impacts of large-scale wind farms on land surface temperature. *Renew. Sustain. Energy Rev.* **16**, 6432–6437 (2012).
33. P. Denholm *et al.*, Land-Use Requirements of Modern Wind Power Plants in the United States. DOE Tech. Rep. NREL/TP-6A2-45834, 2009; [www.nrel.gov/docs/fy09osti/45834.pdf](http://www.nrel.gov/docs/fy09osti/45834.pdf)
34. O. Deschênes, M. Greenstone, Climate Change, Mortality, and Adaptation: Evidence from Annual Fluctuations in Weather in the US. *Am. Econ. J. Appl. Econ.* **3**, 152–185 (2011).
35. M. B. Christiansen, C. B. Hasager, Wake effects of large offshore wind farms identified from satellite SAR. *Remote Sens. Environ.* **98**, 251–268 (2005).
36. M. Z. Jacobson, C. L. Archer, W. Kempton, Taming hurricanes with arrays of offshore wind turbines. *Nat. Clim. Change.* **4**, 195–200 (2014).
37. A. Possner, K. Caldeira, Geophysical potential for wind energy over the open oceans. *Proc. Natl. Acad. Sci. U.S.A.*, **114**, 11338–43 (2017).
38. R. H. Moss *et al.*, The next generation of scenarios for climate change research and assessment, *Nature* **463**, 747–756 (2010).
39. K. L. Ricke, K. Caldeira, Maximum warming occurs about one decade after a carbon dioxide emission. *Environ. Res. Lett.* **9**, 124002 (2014).
40. A. V. Karmalkar *et al.*, Consequences of global warming of 1.5 °C and 2 °C for regional temperature and precipitation changes in the Contiguous United States. *PloS One.* **12**, e0168697 (2017).
41. G. F. Nemet, Net Radiative Forcing from Widespread Deployment of Photovoltaics. *Environ. Sci. Technol.* **43**, 2173–2178 (2009).

**Acknowledgements**

We thank A. Karmalkar for providing ensemble mean surface temperature data for the IPCC RCP4.5 and RCP8.5 projections (40), and S. Leroy and N. Brunsell for technical assistance. This work was supported by the Fund for Innovative Climate and Energy Research.

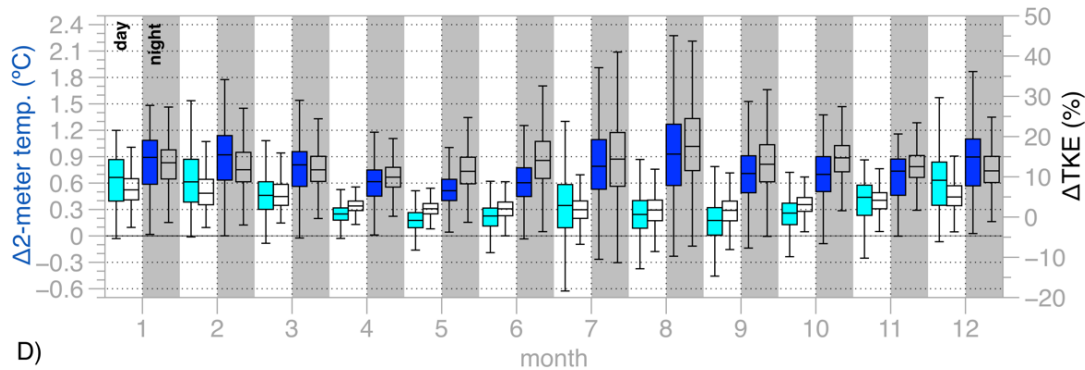
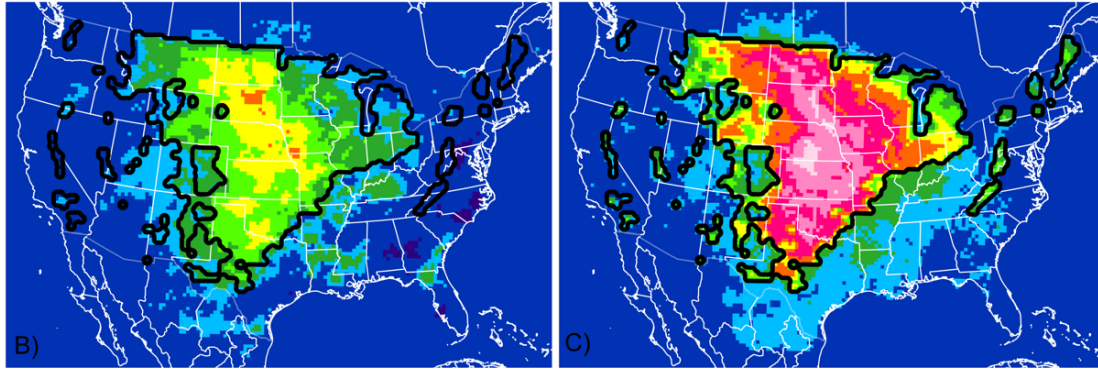
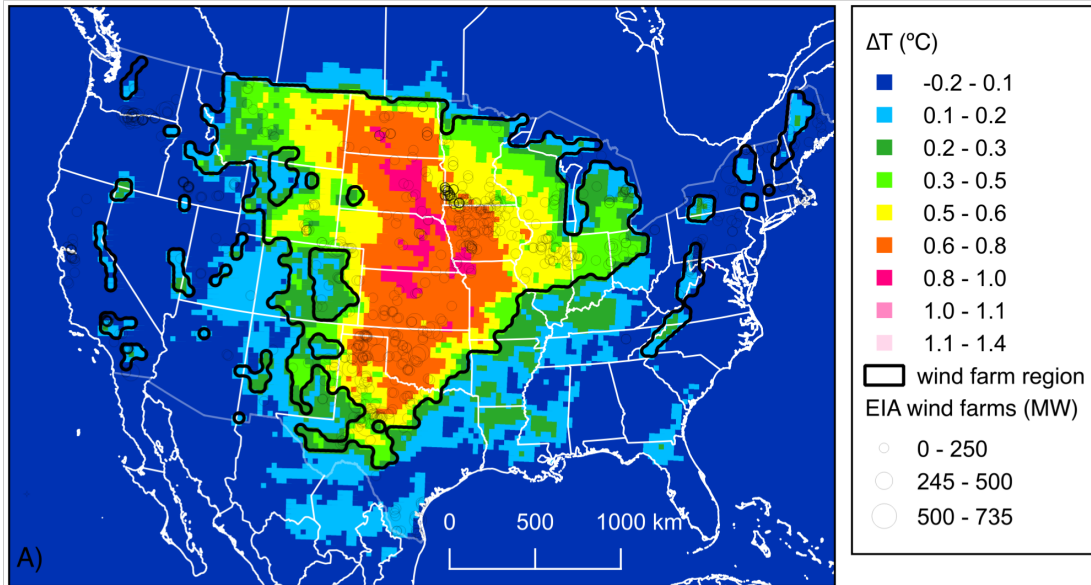


Figure 1: Temperature response to benchmark ( $0.5 \text{ MW km}^{-2}$ ) wind power deployment. Maps are 3-year mean of perturbed minus 3 years of control for 2-meter air temperatures, showing (A) all time periods, (B) daytime, and (C) nighttime. The wind farm region is outlined in black, and, for reference, presently operational wind farms shown as open circles in (A); (D) Monthly day and night differences over the wind farm region for the same 2-meter air temperature differences (solid colored boxes) along with turbulent kinetic energy (TKE) from 0-56 m (transparent boxes), with the vertical line extent showing the standard  $1.5 \cdot$  interquartile range and the box representing the 25th, 50th, and 75th percentiles.

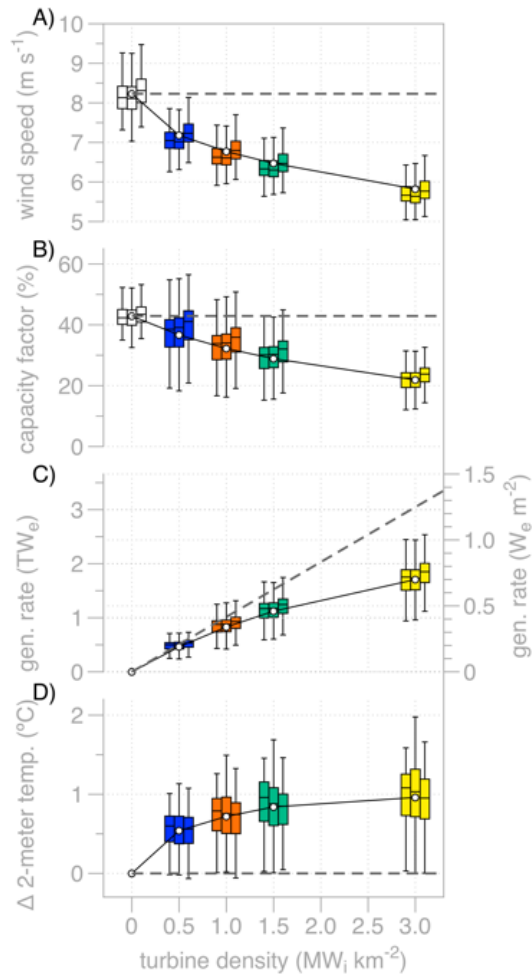


Figure 2. Variation in mean response to changes in wind turbine density over the wind farm region, including (A) 84 m hub-height wind speed, (B) capacity factor, (C) generation rate as a sum and per unit area, and (D) difference in 2-meter air temperature. For each value, three distinct years of data (2012-14 from left to right) are shown as 3 boxplots (1.5 · interquartile range, with 25<sup>th</sup>, 50<sup>th</sup>, 75<sup>th</sup>). Colors help distinguish and group identical turbine densities. The 3-year mean is shown using white points and connecting solid lines. Dashed lines illustrate the expected results if climate did not respond to the deployment of wind turbines.

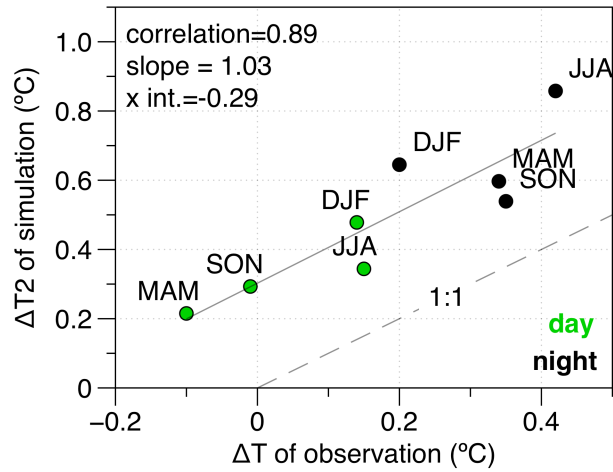


Fig. 3. Comparison of observations and simulations for the Texas location (Table 1). We compare day and night response over four seasons. Observations are surface (skin) temperature differences. Simulation is differences in 2-meter air temperatures between the benchmark scenario ( $0.5 \text{ MW km}^{-2}$ ) and control. Note that while correlation over eight points is high, the simulated response is larger, likely due to the much larger perturbed area and the difference between skin and 2 m air temperature.

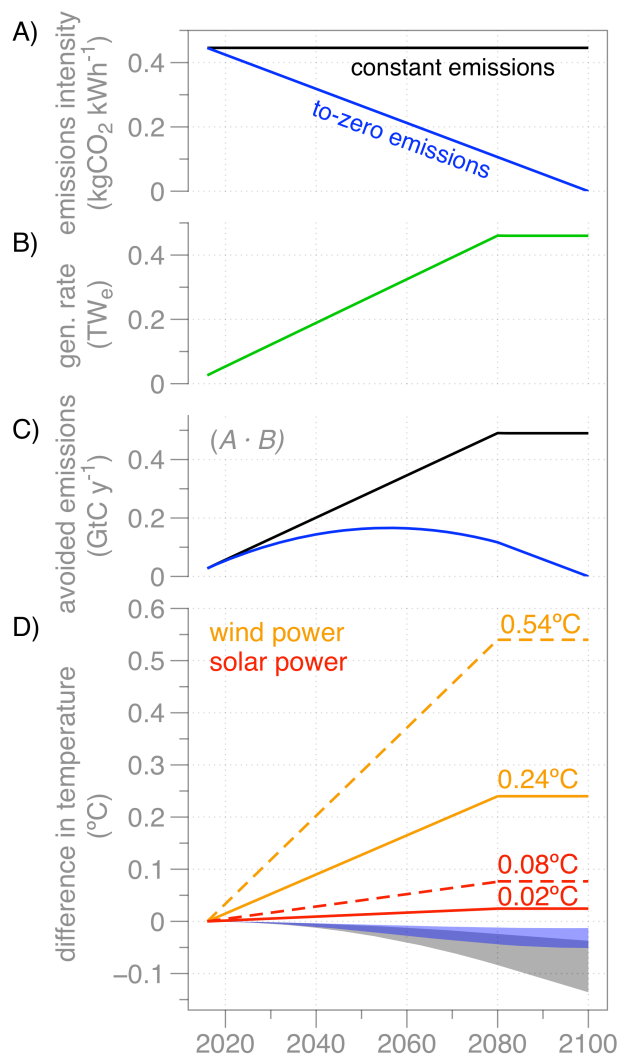


Fig. 4: Comparing the climatic impacts to climate benefits of progressively implementing the *benchmark scenario*, into two pathways (black = constant emissions; blue=to-zero emissions by 2100); **A**) emissions intensity of US electricity generation, **B**) progressive realization of the benchmark scenario's full generation rate by 2080, **C**) emissions avoided (*i.e.*  $A \cdot B$ ), **D**) 2-meter temperature differences within the wind farm region (dotted line) and the Continental US (solid line), as well as the avoided warming from the avoided emissions of (C), with the blue region representing the pathway to-zero emissions and the gray region representing the pathway of static emissions. The range of avoided warming for each pathways is estimated from the min- and max-values within the emissions-to-climate impulse response function.

Table 1. Overview of observational studies linking air temperature differences to wind farms. SAT indicates satellite-based, and GND indicates ground-based observations. Note that measurements identified as the same state were completed over the same wind farms.

Reference	SAT or GND	Period	State	Notes: climatic impacts within or very near to the operational wind farm
Baidya Roy & Traiteur (2010)	GND	53d	CA	summer; ~1°C increase in 5m air temperature downwind at night through the early morning; slight cooling effect during the day
Walsh-Thomas et al. (2012)	SAT	-	CA	~2°C warmer skin temperatures extending to about 2km downwind, with visible temperature differences to 12km downwind
Zhou et al. (2012)	SAT	9y	TX	JJA night=+0.72°C, DJF night=+0.46°C; JJA day=-0.04°C; DJF day=+0.23°C; warming is spatially consistent with the arrangement of wind turbines
Zhou et al. (2013)	SAT	6y	TX	QA1 values: DJF night=+0.22°C, MAM night=+0.29°C, JJA night=+0.35°C, SON night=0.40°C, DJF day=+0.11°C, MAM day=-0.11°C, JJA day=+0.17°C, SON day=-0.04°C
Zhou et al. (2013)	SAT	2y	TX	QA1 values: DJF night=-0.01°C, MAM night=+0.42°C, JJA night=+0.67°C, SON night=0.47°C, DJF day=+0.14°C, MAM day=-0.42°C, JJA day=+1.52°C, SON day=+0.12°C
Xia et al. (2015)	SAT	7y	TX	DJF night=+0.26°C, MAM night=+0.40°C, JJA night=+0.42°C, SON night=+0.27°C, Annual night=+0.31°C, DJF day=+0.18°C, MAM day=-0.25°C, JJA day=-0.26°C, SON day=-0.02°C, Annual day=-0.09°C
Harris et al. (2014)	SAT	11y	IA	MAM night=+0.07°C, JJA night=+0.17°C, SON night=+0.15°C
Rajewski et al. (2013)	GND	122d	IA	along the edge of a large wind farm directly downwind of ~13 turbines; generally cooler temperatures (0.07°C) with daytime periods that were 0.75°C cooler and nighttime periods that were 1.0-1.5°C warmer
Rajewski et al. (2014)	GND	122d	IA	along the edge of a large wind farm downwind of ~13 turbines co-located with corn and soybeans; night sensible heat flux and CO <sub>2</sub> respiration increase 1.5-2 times and wind speeds decrease by 25-50%; daytime H <sub>2</sub> O and CO <sub>2</sub> fluxes increase five-fold 3-5 diameters downwind
Slawsky et al. (2015)	SAT	11y	IL	DJF night=+0.39°C, MAM night=+0.27°C, JJA night=+0.18°C, SON=+0.26°C; Annual=+0.26°C
Smith et al. (2015)	GND	47d	confidential	spring; nighttime warming of 1.9°C downwind of a ~300 turbine wind farm